

Dear Author

Please use this PDF proof to check the layout of your article. If you would like any changes to be made to the layout, you can leave instructions in the online proofing interface. First, return to the online proofing interface by clicking "Edit" at the top of the page, then insert a Comment in the relevant location. Making your changes directly in the online proofing interface is the quickest, easiest way to correct and submit your proof.

Please note that changes made to the article in the online proofing interface will be added to the article before publication, but are not reflected in this PDF proof.

If you would prefer to submit your corrections by annotating the PDF proof, please download and submit an annotatable PDF proof by clicking the button below.

 [Annotate PDF](#)

We have presented the Graphical Abstract text and image for your article below. This brief summary of your work will appear in the contents pages of the issue in which your article appears.

1

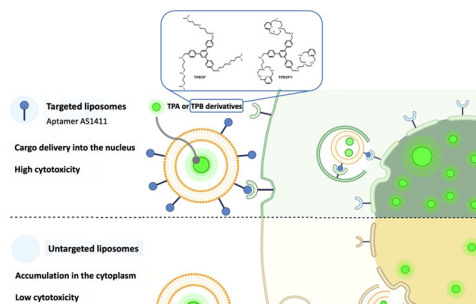
Development of potent tripodal G-quadruplex DNA binders and their efficient delivery to cancer cells by aptamer functionalised liposomes

Isabel Pont, Cristina Galiana-Roselló, María Sabater-Arcis, Ariadna Bargiela, Juan Carlos Frías, M. Teresa Albelda, Jorge González-García* and Enrique García-España*

Trisubstituted TPA/TPB-based ligands containing open-chain and macrocyclic polyamines have a strong G-quadruplex DNA stabilisation effect along with a good selectivity for G4 over duplex DNAs although they exhibit

Q5 low cytotoxicity in cancer cells. This limitation is overcome

Q6 by their encapsulation in liposomes and AS1411 aptamer-targeted liposomes reaching nanomolar IC_{50} values.



Please check this proof carefully. Our staff will not read it in detail after you have returned it.

Please send your corrections either as a copy of the proof PDF with electronic notes attached or as a list of corrections. **Do not edit the text within the PDF or send a revised manuscript** as we will not be able to apply your corrections. Corrections at this stage should be minor and not involve extensive changes.

Proof corrections must be returned as a single set of corrections, approved by all co-authors. No further corrections can be made after you have submitted your proof corrections as we will publish your article online as soon as possible after they are received.

Please ensure that:

- The spelling and format of all author names and affiliations are checked carefully. You can check how we have identified the authors' first and last names in the researcher information table on the next page. **Names will be indexed and cited as shown on the proof, so these must be correct.**
- Any funding bodies have been acknowledged appropriately and included both in the paper and in the funder information table on the next page.
- All of the editor's queries are answered.
- Any necessary attachments, such as updated images or ESI files, are provided.

Translation errors can occur during conversion to typesetting systems so you need to read the whole proof. In particular please check tables, equations, numerical data, figures and graphics, and references carefully.

Please return your **final** corrections, where possible within **48 hours** of receipt, by e-mail to: obc@rsc.org. If you require more time, please notify us by email.

Funding information

Providing accurate funding information will enable us to help you comply with your funders' reporting mandates. Clear acknowledgement of funder support is an important consideration in funding evaluation and can increase your chances of securing funding in the future.

We work closely with Crossref to make your research discoverable through the Funding Data search tool (<http://search.crossref.org/funding>). Funding Data provides a reliable way to track the impact of the work that funders support. Accurate funder information will also help us (i) identify articles that are mandated to be deposited in **PubMed Central (PMC)** and deposit these on your behalf, and (ii) identify articles funded as part of the **CHORUS** initiative and display the Accepted Manuscript on our web site after an embargo period of 12 months.

Further information can be found on our webpage (<http://rsc.li/funding-info>).

What we do with funding information

We have combined the information you gave us on submission with the information in your acknowledgements. This will help ensure the funding information is as complete as possible and matches funders listed in the Crossref Funder Registry.

If a funding organisation you included in your acknowledgements or on submission of your article is not currently listed in the registry it will not appear in the table on this page. We can only deposit data if funders are already listed in the Crossref Funder Registry, but we will pass all funding information on to Crossref so that additional funders can be included in future.

Please check your funding information

The table below contains the information we will share with Crossref so that your article can be found *via* the Funding Data search tool. **Please check that the funder names and grant numbers in the table are correct and indicate if any changes are necessary to the Acknowledgements text.**

Funder name	Funder's main country of origin	Funder ID (for RSC use only)	Award/grant number
Federación Española de Enfermedades Raras	Spain	501100002924	Unassigned
Conselleria de Innovación, Universidades, Ciencia y Sociedad Digital, Generalitat Valenciana	Spain	501100016386	CIDEGENT/2018/015 CIPROM/2021/030
Ministerio de Ciencia e Innovación	Spain	501100004837	CEX2019-000919 MFA/2022/014 PID2019-108643GA-I00 PID2019-110751RB-I00 RED2018-102331-T
European Cooperation in Science and Technology	Belgium	501100000921	CA18202

Q1

Researcher information

Please check that the researcher information in the table below is correct, including the spelling and formatting of all author names, and that the authors' first, middle and last names have been correctly identified. **Names will be indexed and cited as shown on the proof, so these must be correct.**

If any authors have ORCID or ResearcherID details that are not listed below, please provide these with your proof corrections. Please ensure that the ORCID and ResearcherID details listed below have been assigned to the correct author. Authors should have their own unique ORCID iD and should not use another researcher's, as errors will delay publication.

Please also update your account on our online [manuscript submission system](#) to add your ORCID details, which will then be automatically included in all future submissions. See [here](#) for step-by-step instructions and more information on author identifiers.

First (given) and middle name(s)	Last (family) name(s)	ResearcherID	ORCID iD
Isabel	Pont		
Cristina	Galiana-Roselló		
Maria	Sabater-Arcis		
Ariadna	Bargiela		
Juan Carlos	Frías		
M. Teresa	Albelda		
Jorge	González-García	R-5481-2017	0000-0001-8994-1779
Enrique	García-España		0000-0002-4601-6505

Queries for the attention of the authors

Journal: **Organic & Biomolecular Chemistry** Paper: **d2ob01911f**

Title: **Development of potent tripodal G-quadruplex DNA binders and their efficient delivery to cancer cells by aptamer functionalised liposomes**

For your information: You can cite this article before you receive notification of the page numbers by using the following format: (authors), Org. Biomol. Chem., (year), DOI: 10.1039/d2ob01911f.

Editor's queries are marked like this **Q1**, **Q2**, and for your convenience line numbers are indicated like this 5, 10, 15, ...



Please ensure that all queries are answered when returning your proof corrections so that publication of your article is not delayed.

Query Reference	Query	Remarks
Q1	Funder details have been incorporated in the funder table using information provided in the article text. Please check that the funder information in the table is correct and indicate any changes, if required. If changes are required, please ensure that you also amend the Acknowledgements text as appropriate.	
Q2	The article title has been altered for clarity. Please check that the meaning is correct.	
Q3	Have all of the author names been spelled and formatted correctly? Names will be indexed and cited as shown on the proof, so these must be correct. No late corrections can be made.	
Q4	Do you wish to add an e-mail address for the corresponding author? If so, please provide the relevant information.	
Q5	The GA text has been altered for clarity. Please check that the meaning is correct.	
Q6	The Graphical Abstract text currently exceeds the space available for the published version. Please trim the text so that it is shorter than 250 characters (including spaces).	
Q7	The sentence beginning "The ligands hold three..." has been altered for clarity. Please check that the meaning is correct.	
Q8	The sentence beginning "Furthermore, liposomes are ..." has been altered for clarity. Please check that the meaning is correct.	
Q9	The meaning of the phrase "attending" in the sentence beginning "Attending to the chemical structures..." is not clear - please provide alternative text.	
Q10	The sentence beginning "Then, LN229 cells ..." has been altered for clarity. Please check that the meaning is correct.	
Q11	The sentence beginning "In light of these ..." has been altered for clarity. Please check that the meaning is correct.	

Q12	The sentence beginning "The mass spectrometry analysis ..." has been altered for clarity. Please check that the meaning is correct.	
Q13	Have all of the funders of your work been fully and accurately acknowledged? If not, please ensure you make appropriate changes to the Acknowledgements text.	
Q14	Please check that ref. 6c has been displayed correctly.	
Q15	Ref. 7a: Please provide the year of publication.	
Q16	Please check that ref. 9b has been displayed correctly.	
Q17	Please check that ref. 18a has been displayed correctly.	

PAPER

Development of potent tripodal G-quadruplex DNA binders and their efficient delivery to cancer cells by aptamer functionalised liposomes†

Isabel Pont,^a Cristina Galiana-Roselló,^a Maria Sabater-Arcis,^{b,c,d} Ariadna Bargiela,^e Juan Carlos Frías,^f M. Teresa Albelda,^a Jorge González-García ^{*a} and Enrique García-España ^{*a}

Two new ligands (**TPB3P** and **TPB3Py**) showing a strong stabilisation effect and good selectivity for G4 over duplex DNAs have been synthesised. The ligands hold three analogous polyamine pendant arms (**TPA3P** and **TPA3Py**) but differ in the central aromatic core, which is a triphenylbenzene moiety instead of a triphenylamine moiety. Both **TPB3P** and **TPB3Py** exhibit high cytotoxicity in MCF-7, LN229 and HeLa cancer cells in contrast to TPA-based ligands, which exhibit no significant cytotoxicity. Moreover, the most potent G4 binders have been encapsulated in liposomes and AS1411 aptamer-targeted liposomes reaching nanomolar IC₅₀ values for the most cytotoxic systems.

Received 19th October 2022,
Accepted 12th December 2022

DOI: 10.1039/d2ob01911f

rsc.li/obc

Introduction

Modern medicinal chemistry involves the discovery and targeting of novel disease modulators such as histone modifications, nucleosome remodelers, modified DNA/RNA bases and a variety of non-coding mediating elements.¹ One of the most attractive non-coding targets for cancer and neurodegenerative therapies are G-quadruplex structures (G4s).² G4s are non-canonical nucleic acid structures formed by guanine-rich sequences from both DNA and RNA. These structures are formed by two or more stacked G-quartet units, which are planar rearrangements of four guanine bases held together by a hydrogen bonding network between the Hoogsteen and Watson-Crick faces of the guanines.³ Within the central channel of G4s, cations such as sodium and potassium undergo several dipole interactions to assemble the final structure. Next generation sequencing and bioinformatic analysis have located putative G-quadruplex forming sequences in

human telomeres, oncogene-promoter regions, replication initiation sites and untranslated regions.⁴ The formation of G-quadruplexes under pathophysiological conditions has been associated with the regulation of important cancer biology processes such as oncogene expression, telomere maintenance and chromosome stability.⁵ A large number of G4 binders have been described in the last few years which can act as anti-cancer agents⁶ but only three molecules have progressed to clinical trials, namely Quarfloxin (CX-3543), CX-5461 and APTO253.⁷

The rational design of G4 binders is based on the G4-ligand structures available in databases, in which an extended poly-aromatic π -deficient core is selected to bind on the G-tetrad and hamper duplex intercalation.⁸ Because of the scarce solubility of these scaffolds, the incorporation of positively charged moieties into the G4-ligand structure is sought to enhance the aqueous solubility with the possibility of further establishing electrostatic and hydrogen bond interactions with the phosphates and nucleobases or bridges with the water molecules hosted within the grooves.⁹ According to these features, G4 binders have been developed and can be classified into several categories based on their structure such as acridines, perylenes, anthraquinones, porphyrins or metal complexes.¹⁰ Among them, tripodal molecules such as triarylpyridines and terpyridines have been reported as potent quadruplex binders selective for G4s over duplex DNA.¹¹ Recently, the triarylamine fluorescent probe 4,4',4''-(nitriлотris(benzene-4,1-diyl))tris(1-ethylpyridin-1-ium) iodide (**NBTE**) has been shown to bind two guanines of the G-tetrad inducing a binding pocket at the 5' end of the G4.¹²

^aInstituto de Ciencia Molecular (ICMol), Departamento de Química Inorgánica, Universidad de Valencia, Catedrático José Beltrán 2, 46980 Paterna, Spain

^bTranslational Genomics Group, Incliva Health Research Institute, Valencia, Spain

^cInterdisciplinary Research Structure for Biotechnology and Biomedicine (ERI BIOTECMED), University of Valencia, Valencia, Spain

^dCIPF-INCLIVA Joint Unit, Valencia, Spain

^eNeuromuscular Research Unit, Neurology Department, Hospital La Fe, Instituto de Investigación Sanitaria La Fe (IISLAFE), Valencia, Spain

^fDepartment of Biomedical Sciences, CEU Cardenal Herrera University, Ramón y Cajal s/n, 46115 Alfara del Patriarca, Spain

† Electronic supplementary information (ESI) available. See DOI: <https://doi.org/10.1039/d2ob01911f>

Despite the advances in the design and development of potent and selective G4 binders, cell factors and conditions as well as their low accumulation in cells hinder the interaction of the molecules with G4s.¹³ To overcome these issues, drug delivery systems which can selectively accumulate G4 ligands in cells have been proposed to improve their therapeutic efficacy.¹⁴

Drug delivery systems have become an integral tool in research and clinical applications to administer drugs, and enhance their therapeutic effect with improved biodistribution.¹⁵ Among the drug delivery systems, liposomes constitute one of the best-known and widely used systems since the early 1970s.¹⁶ The translation from the bench to the clinic was successfully achieved with the drug-loaded liposomal system Doxil®, which allows, with less cardiotoxicity, a more efficient accumulation of the drug doxorubicin in ovarian and breast tumours than when using a non-liposomal approach.¹⁷ Since then, several liposomal drug formulations have been either approved by the FDA or are currently in late-stages of clinical trials.¹⁸ The advantages of using liposomes for drug delivery include enhancement of the drug solubility, resistance to the enzymatic degradation of the loaded drug, and minimisation of side-effects and toxicity.¹⁹ Furthermore, liposomes are an excellent platform to design and build multimodal systems using simple, low cost and scalable synthesis methods. Having this in mind, some of us reported fumagillin-loaded liposomes for the early treatment of atherosclerotic plaques, which reduced the lesion size after 5-weeks of treatment in a murine model.²⁰

Recently, our team has launched a project to develop G4 DNA binders based on the triphenylamine (TPA) scaffold, an appropriate moiety for stacking on top of G4s.²¹ Some of the ligands showed high affinity and a strong stabilisation effect for G4s. Herein, we have explored the substitution of the triphenylamine moiety for the more rigid triphenylbenzene unit, and we have evaluated the interaction with G4s. Moreover, we have assessed the biological activity and we have encapsulated the ligands into liposomes to enhance the cytotoxic effect of the best G4 binders.

Results and discussion

Initial biological assessment

We designed TPA-based molecules having one, two or three appended linear or macrocyclic polyamine substituents (Fig. 1A and S1–S6†) and we studied their affinity and stabilisation towards a panel of G4s.^{22,23} We found that the trisubstituted TPA-based ligands (**TPA3P** and **TPA3Py**, Fig. 1 and S9†) have the highest affinity and strongest stabilisation effect for G4s. Moreover, the open-chain derivative **TPA3P** has an excellent selectivity for G4s over duplex DNA (Fig. 1).²³ In order to assess the biological activity, we have evaluated the cell viability of the previously reported G4 binders in MCF-7, LN229 and HeLa cancer cells (see Fig. 1B). Interestingly, the best G4 binder **TPA3P** ($K_a \sim 10^6 \text{ M}^{-1}$ and $\Delta T_m \sim 25 \text{ }^\circ\text{C}$ for the HTelo

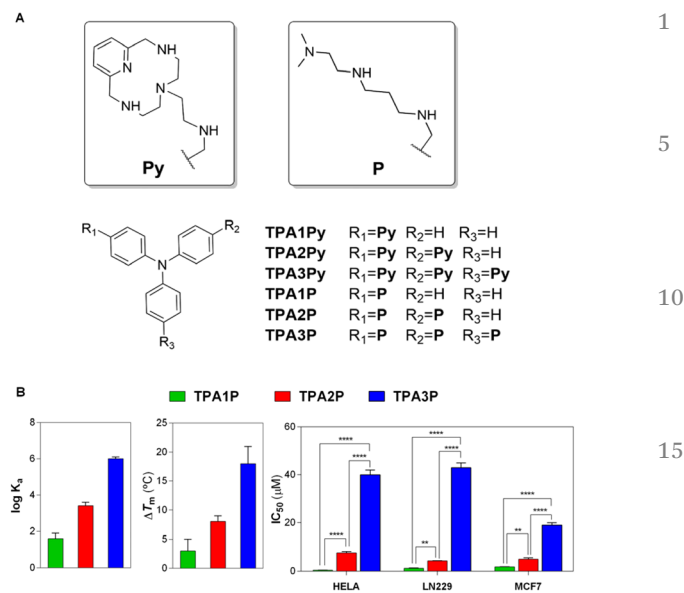


Fig. 1 (A) Structures of TPA-based molecules under study. (B) Values of $\log K_a$ and ΔT_m ($^\circ\text{C}$) for HTelo and IC_{50} (μM) obtained from fluorimetric titrations, FRET melting and viability assays, respectively. Fluorimetric and FRET melting assays were conducted in 10 mM LiCac buffer supplemented with 100 mM KCl, pH 7.2. Viability assays were conducted at 24 h of ligand incubation. See the Experimental section for details. Data compiled from ref. 22 and 23.

G-quadruplex, Fig. 1) possesses the lowest cytotoxicity values (highest IC_{50}) in all cell lines ($\text{IC}_{50} > 20 \mu\text{M}$). Both **TPA1P** and **TPA2P** show cytotoxicity in the low micromolar range, having IC_{50} values ranging from 0.4 to 7.7 μM depending on the cell line. However, the monosubstituted binder **TPA1P** has higher cytotoxicity than **TPA2P**. These results are apparently in contradiction with the binding affinity for the G4s (Fig. 1); the trisubstituted **TPA3P** binder having the highest affinity should have shown the highest cytotoxicity. Similar features were obtained for the derivatives with the macrocyclic substituents (Fig. S9†). This fact may be ascribed to the net charge of the molecules at the physiological pH of 7.4, since the highly substituted molecules, which are more charged at this pH, may be unable to cross the cellular membrane.

Synthesis of new tripodal G4 ligands and evaluation of the G4 interaction and cytotoxicity

Having in mind that the trisubstituted ligands are the most promising G4 binders *in vitro*, we have synthesised two new molecules containing three either linear or macrocyclic pendant substituents but with a 1,3,5-triphenylbenzene moiety as the central core instead of a triphenylamine moiety (**TPB3P** and **TPB3Py**, Fig. 2).

These new molecules possess a larger aromatic surface to interact with a G-tetrad but avoid the central amine atom, which should facilitate a more efficient planar arrangement. In addition, they can show different pharmacological properties which may improve their cytotoxic effect in cancer cells. The ligands were synthesised using a similar protocol to that used

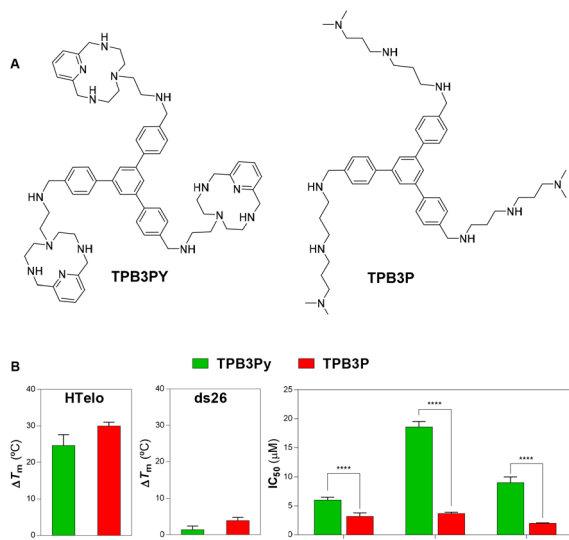


Fig. 2 (A) Structures of TPB-based molecules under study. (B) Values of ΔT_m (°C) for HTelo and ds26 and IC_{50} (μM) obtained from FRET melting and viability assays, respectively. FRET melting assays were conducted in 10 mM LiCac buffer supplemented with 100 mM KCl, pH 7.2. Viability assays were conducted at 24 h of ligand incubation. See the Experimental section for details.

for TPA ligands (see Materials and instrumentation) and their characterisation is shown in the ESI (Fig. S7 and S8†).

Once the ligands were obtained, we conducted FRET melting experiments to assess the G4 interaction. Both ligands showed a strong stabilisation effect in the HTelo G-quadruplex ($\Delta T_m = 30$ and 24.6 °C for **TPB3P** and **TPB3Py** respectively, Fig. 2), confirming a strong interaction with G4s. Then, we evaluated the stabilisation effect on a duplex model (*i.e.* ds26) and no significant variation of the melting temperature was observed ($\Delta T_m = 3.9$ and 1.4 °C for **TPB3P** and **TPB3Py** respectively, Fig. 2), suggesting a high selectivity for G4 over duplex structures, similar to the tripodal TPA-based analogues **TPA3P** and **TPA3Py**. However, both ligands exhibited lower IC_{50} values than their triphenylamine analogues for all the studied cancer cell lines (see Fig. 2). The tripodal ligand with the macrocyclic substituents (**TPB3Py**) shows between 1.3 and 7-fold decrease in the values of IC_{50} depending on the cell line in comparison with the TPA analogue (**TPA3Py**). Strikingly, **TPB3P** exhibits an even higher cytotoxicity, presenting a 10-fold decrease in the IC_{50} values when compared to **TPA3P**. Attending to the chemical structures, the pendant arms affect the interaction with DNA but the central aromatic core modulates the effect in cells. We hypothesise that the larger hydrophobicity of the TPB moiety in comparison with the TPA moiety increases the cellular uptake and thus the cytotoxicity.

Liposomal development

In the light of these results, we attempted to obtain a better correlation between the G4 stabilisation and the cytotoxicity of the TPA/TPB derivatives. Therefore, we developed a novel strategy to target DNA G4s in cancer cells using a liposomal-based

system. We encapsulated the most promising G4 binders, which should be the most cytotoxic agents (**TPA3P**, **TPA3Py**, **TPB3P** and **TPB3Py**), into liposome nanoparticles with the aim to increase their cellular uptake (**TPA3P-Lip**, **TPA3Py-Lip**, **TPB3P-Lip** and **TPB3Py-Lip**, termed non-targeted liposomes). Furthermore, in order to specifically target cancer cells and enhance the cargo delivery of the compounds into the nucleus, we incorporated the DNA aptamer AS1411 (**TPA3P-Lip + Apt**, **TPA3Py-Lip + Apt**, **TPB3P-Lip + Apt** and **TPB3Py-Lip + Apt**, termed targeted liposomes) within the membrane of the liposomes (Fig. 3).²⁴ AS1411 is well known to interact with the nucleolin receptor,²⁵ which is overexpressed on the surface of cancer cells. These nanoscale constructions are termed liposomal spherical nucleic acids, which lead to a high cellular internalisation in addition to hampering the nuclease degradation of the aptamers and transcytose across different biological barriers.²⁶ Of note, AS1411 folds into a G-quadruplex structure, which can potentially bind the ligands when incorporated into the liposomes.²⁷ Having the possibility to design our own drug delivery system, we additionally functionalised the liposomes with the fluorescent phospholipid **DPPE-NBD** (dipalmitoylphosphatidylethanolamine–nitrobenzoxadiazole) for fluorescence visualisation. The resulting systems can be described as multimodal drug-delivery/imaging or theranostic systems.

The liposomes were prepared by lipid film hydration (see the Experimental section). We additionally PEGylated the liposomes to increase the serum stability with DSPE-mPEG2000.²⁸ Then, we assessed the characteristics of the liposomes such as size, polydispersity and encapsulation efficiency. Control liposomes were also prepared without the AS1411 aptamer. The average size and size distribution of liposomes were characterised by dynamic light scattering (DLS) (Table S1 and Fig. S10†). The aptamer-functionalised liposomes showed an average diameter of 124 nm, while the control ones had a lower hydrodynamic diameter of 95 nm. These results indicated that the liposomal size increased due to the AS1411 functionalisation. Taking advantage of the presence of the nitrobenzoxadiazole fluorophore (**DPPE-NBD**), vesicle formation of the liposome suspensions was visualised by confocal laser scanner microscopy ($\lambda_{exc} = 463$ nm, $\lambda_{em} = 536$ nm). Liposomes were formed as bright green spheroids continuously moving in solution (Fig. S11†).

Finally, the encapsulation efficiency was quantified by using the intrinsic fluorescence emission of the ligands. We

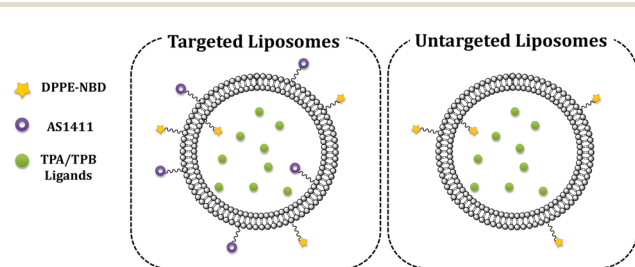


Fig. 3 Schematic representation of liposomal nanoparticles.

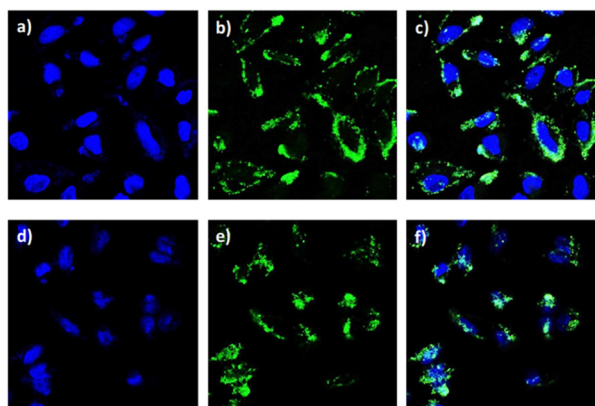


Fig. 4 Representative confocal microscopy images of live LN229 cells treated with Lip (a, b and c) and Lip + Apt (d, e and f). LN229 cells were treated with the liposomal formulations at 37 °C for 1 hour. Then, they were incubated with Hoechst 33342 at 37 °C for 30 minutes. Blue nuclear stain, Hoechst filter (a and d), green stain, NBD filter (b and e) and merging of both channels (c and f).

plotted a standard calibration curve of the fluorescence emission of the compounds in a MeOH : H₂O mixture (90 : 10 V : V) using excitation/emission wavelengths of the molecules ($\lambda_{\text{exc}} = 314$ nm, $\lambda_{\text{em}} = 370$ nm, Fig. S12[†]). Liposome nanoparticles lacking the DPPE-NBD phospholipid were diluted with MeOH : H₂O solution (90 : 10 V : V) to disrupt the vesicle membrane and release the molecular cargo. The concentrations of TPA3P, TPA3Py, TPB3P and TPB3Py of the liposome formulations are compiled in Table S2.[†]

To gain further insight into the cellular localisation and cargo delivery of the liposomes, we monitored the fluorescence emission in live cells by confocal laser scanning microscopy.

We firstly investigated the fluorescence emission of the G4 binders at different incubation times and concentrations by confocal microscopy, although no signal was detected due to the lack of brightness of the G4 binders at the lower excitation channel of the microscope ($\lambda_{\text{exc}} = 405$ nm). Then, LN229 cells were incubated for 1 hour until the liposomes were depleted of the compounds to avoid cell death (Lip). Several images were obtained in the green channel showing the fluorescence of the NBD molecules attached to the liposomal membranes (Fig. 4). Specifically, these images showed emission only in the cytoplasmic region; the liposomes seemed to stick to the nuclear membrane without entering the nucleus. However, the liposome formulations including the aptamer moiety, Lip + Apt, showed fluorescence emission in both the cytoplasmic and nuclear regions, resulting in an overlapping between the NBD emission and the Hoechst-stained nucleus (Fig. 4 and S13 and S14 in the ESI[†]).

Cytotoxicity of liposomal systems

Once the liposomes had been characterised, we assessed their therapeutic potential to target cancer cells using the MTT assay. We conducted the assays with three different cancer cell lines, namely MCF-7, LN229 and HeLa from breast, glioblastoma and cervical tumours, respectively. The values of the half-maximal inhibitory concentration (IC₅₀) are presented in Table 1 and Fig. 5. The dose-response curves are included in the ESI (Fig. S15[†]). Of note, both liposome-unloaded systems (targeted and non-targeted) have no cytotoxicity suggesting that the aptamer AS1411 acts only as a controller of the cargo delivery.

Interestingly, the liposome-loaded systems produced enhancements of the cytotoxicity in the cancer cell lines from 20 to 40-fold for TPA3P-Lip and from 160 to 301-fold for

Table 1 IC₅₀ (μM) values for the different systems studied and IC₅₀ ratios between liposomal formulations and free compounds

Cell line	TPA3P [1]	TPA3P-Lip [2]	TPA3P-Lip + Apt [3]	[1]/[2]	[1]/[3]
LN229	43(2) ^a	1.053(6)	0.205(6)	40	113
MFC-7	19(1)	0.98(3)	0.109(6)	19	211
HeLa	40(2)	1.40(2)	0.109(7)	29	366
	TPA3Py [1]	TPA3Py-Lip [2]	TPA3Py-Lip + Apt [3]	[1]/[2]	[1]/[3]
LN229	24.4(6)	0.152(6)	0.054(3)	160	452
MFC-7	19(1)	0.130(8)	0.053(2)	146	360
HeLa	47(2)	0.156(5)	0.053(5)	301	887
	TPB3P [1]	TPB3P-Lip [2]	TPB3P-Lip + Apt [3]	[1]/[2]	[1]/[3]
LN229	3.7(2)	0.66(9)	0.072(3)	5	51
MFC-7	2.0(1)	0.386(5)	0.051(2)	5	39
HeLa	3.2(6)	0.645(9)	0.063(5)	5	50
	TPB3Py [1]	TPB3Py-Lip [2]	TPB3Py-Lip + Apt [3]	[1]/[2]	[1]/[3]
LN229	18.6(9)	0.27(5)	0.093(7)	69	200
MFC-7	9(1)	0.130(8)	0.086(6)	69	104
HeLa	6.0(5)	0.645(9)	0.058(2)	9	103

^a Values in parentheses are standard deviations in the last significant digit.

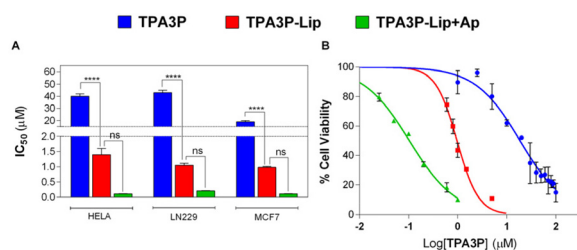


Fig. 5 (A) Values of viability assays (IC₅₀, µM) of the TPA3P, TPA3P-Lip and TPA3P-Lip + Apt systems. (B) Curves of dose-response of TPA3P, TPA3P-Lip and TPA3P-Lip + Apt systems for the MCF-7 cancer cell line. Data are expressed as mean ± SD (*n* = 3 independent assays).

TPA3Py-Lip with respect to the non-encapsulated molecules. The cytotoxicity of the liposomes charged with TPB-based ligands increased only 5-fold for TPB3P-Lip and from 10 to 70-fold for TPB3Py-Lip with respect to the free ligands.

The aptamer-functionalised liposomes showed further increases in cytotoxicity from 113-fold to 366-fold for TPA3P-Lip-Apt, and from 452- to 887-fold for TPA3Py-Lip-Apt with respect to the free binders. The TPB3P systems decorated with aptamers exhibited enhancements from 40 to 50-fold for TPB3P-Lip-Apt, whereas TPB3Py-Lip-Apt showed an increase from 100 to 200-fold with respect to free binders. The IC₅₀ values indicate that all the liposome systems containing aptamers have viabilities in the nanomolar range. In light of these results, it can be concluded that the accumulation of non-targeted liposomes in the nuclear membrane shown by confocal microscopy already leads to some drug delivery in the nucleus, which is further enhanced by the aptamer-guided entrance of the liposomes into the nucleus.

Q11

Conclusions

In this work, a family of compounds constituted by the TPA scaffold linked to one, two or three appended either open-chain or macrocyclic polyamine substituents show promising capacity as G-quadruplex binders. However, the most promising G4 binders, TPA3P and TPA3Py, showed less toxicity (higher IC₅₀) towards MCF-7, LN229 and HeLa cancer cells in comparison with the derivatives with one and two polyamine substituents. This fact can be ascribed to the high charge of the trisubstituted binders, which hampered their cellular uptake. To circumvent this limitation, two new ligands were synthesised containing a different tripodal core, *i.e.* the triphenylbenzene moiety, but preserving the three polyamine substituents (TPB3P and TBP3Py). The DNA experiments confirm the high interaction of both molecules and preference for G4s over duplex DNAs as well as an increased cytotoxicity in the three cancer cell lines with respect to the trisubstituted TPA analogues. Moreover, the cell effect limitation may be overcome by the encapsulation of the ligands in liposomes and aptamer-targeted liposomes. The IC₅₀ values decreased markedly for TPA3P-Lip or TPA3Py-Lip and moderately for TPB3P-Lip or

TPB3Py-Lip, showing a further decrease for the aptamer-targeted liposomes (Lip + Ap), reaching, in all cases, nanomolar concentrations. Confocal microscopy studies showed the accumulation of non-targeted liposomes in the proximity of the cell nucleus and the nuclear uptake of the targeted ones. These results point out the potential of modifying the central core of G4 binders as well as the application of the aptamer AS1411 to deliver liposome formulations into the cell nucleus, enhancing the anti-tumour effect of the tripodal compounds.

Experimental

Materials and instrumentation

All reagents were obtained from commercial sources and used without further purification. Phospholipidic molecules were purchased from Avanti Polar Lipids (USA) or NOF (Japan). A dialysis membrane (Spectra/Por®6 Dialysis, MWCO: 2000 Da) was provided by Fisher. HPLC purity grade DNA oligonucleotides were purchased from IDT (Integrated DNA Technologies, Belgium). Mass spectrometry, NMR and elemental experiments were performed at the Central Service for Experimental Science (SCSIE) of the University of Valencia. Deuterated solvents for NMR purposes were obtained from Sigma-Aldrich and used as received. ¹H NMR and ¹³C NMR were recorded on a Bruker Advance 300 spectrometer operating at 300 MHz (¹H) and 75.4 MHz (¹³C). ¹H and ¹³C chemical shifts (δ) were referenced internally to the solvent shift and to the internal standard TMS (D₂O: ¹H δ: 1.94, ¹³C δ: 118.7; acetone-*d*₆: ¹H δ: 2.05, ¹³C δ: 29.7). Chemical shifts have been quoted in ppm, the downfield direction being defined as positive. All NMR data were acquired and processed using Topspin and MestreNova software respectively. The mass spectrometry analysis was performed under an ESI+ condition on a LCT Premier mass spectrometer. UV Vis absorption spectra were recorded on a Varian Cary 100 Bio spectrophotometer and fluorescence emission spectra on a PTI spectrofluorimeter using a microcuvette with *l* = 1 cm. Molecular weights of the ligands were determined using the elemental analysis in tandem with the number of hydrochloride units and solvent molecules calculated from the elemental microanalysis and supported by the study of the acid-base behaviour by means of potentiometric titrations.

Synthesis of the TPB-based compounds

The synthesis of 1,3,5-tris(4-formylphenyl)benzene was conducted by adding tribromobenzene (1.0 g, 3.2 mmol), 4-formylphenylboronic acid (1.5 g, 95.3 mmol) and bis(triphenylphosphine)palladium(II) dichloride (300 mg, 0.4 mmol) to a 1 L round-bottom flask, which was evacuated and backfilled with nitrogen three times. After adding 200 mL of degasified THF, the mixture was heated to reflux for 12 hours under nitrogen. Then, the solution was extracted with CH₂Cl₂ (3 × 50 mL). The organic phase was dried over Na₂SO₄ and evaporated under reduced pressure. The crude product was recrystallized from acetonitrile, obtaining white crystals (TPB-3CHO).²⁹

Q12

1,3,5-Tris(4-formylphenyl)benzene (TPB-3CHO). Yield: 53%; $^1\text{H NMR}$ (300 MHz, CDCl_3): δ = 10.10 (s, 3H), 8.04 (d, J = 8 Hz, 6H), 7.91 (s, 3H), 7.87 (d, J = 9 Hz, 6H). $^{13}\text{C NMR}$ (75.2 MHz, CDCl_3): δ = 191.75, 146.28, 141.59, 135.75, 130.44, 127.98, 126.48 ppm; ESI-MS m/z : 309.1 $[\text{M} + \text{H}]^+$; elemental analysis calcd (%) for $\text{C}_{27}\text{H}_{18}\text{O}_3 \cdot \text{H}_2\text{O}$ (408.13 g mol^{-1}): C 79.4; H 4.9; found: C 79.8; H 5.9.

The functionalisation of the TPB moiety is analogous to the above described with TPA aldehydes. A solution of 1 equivalent of TPB-3CHO in anhydrous CH_2Cl_2 was added dropwise to an anhydrous ethanol solution of 3 equivalents of the polyamine substituent. Then, the mixture was stirred for 12 h under nitrogen. The solvent was removed under reduced pressure and the resulting crude product was treated with water (25 mL) and extracted with CH_2Cl_2 (3×40 mL). The organic phase was dried over Na_2SO_4 and evaporated to afford a yellow oil. Finally, the oily product was dissolved in anhydrous ethanol and precipitated with HCl in dioxane (0.4 M), yielding to the hydrochloride salts of TPB3P or TPB3Py.

1,3,5-Tris{4-[10-methyl-2,6,10-triazaundecaphan-1-yl]phenyl}benzene (TPB3P). Yield: 66%; $^1\text{H NMR}$ (300 MHz, D_2O): δ = 7.85 (s, 3H), 7.78 (d, J = 7 Hz, 6H), 7.54 (d, J = 7 Hz, 6H), 4.27 (s, 6H), 3.21–3.07 (m, 24H), 2.17–2.04 (m, 12H). $^{13}\text{C NMR}$ (75.2 MHz, D_2O): δ = 141.27, 130.49, 130.02, 127.87, 125.15, 54.19, 50.95, 44.68, 44.45, 44.04, 42.80, 22.67, 21.22 ppm; ESI-MS m/z : 820.6 $[\text{M} + \text{H}]^+$; elemental analysis calcd (%) for $\text{C}_{51}\text{H}_{81}\text{N}_9 \cdot 9\text{HCl}$ (1148.41 g mol^{-1}): C 53.3; H 7.9; N 10.9; found: C 53.5; H 8.1; N 10.5.

1,3,5-Tris{4-[3,6,9-triaza-1(2,6)pyridinecyclodecaphan-6-yl]2-azabutyl}benzene (TPB3Py). Yield: 52%; $^1\text{H NMR}$ (300 MHz, MeOD): δ = 7.98 (t, J = 15 Hz), 7.81–7.68 (m, 12 H), 7.54–7.44 (m, 9H), 4.67 (s, 12H), 4.41 (s, 6H), 3.45–3.35 (s, 12H), 3.25–2.85 (s, 24H). $^{13}\text{C NMR}$ (75.2 MHz, MeOD): 149.37, 139.16, 130.66, 127.40, 127.27, 126.87, 121.57, 51.52, 50.58, 50.20, 49.26, 45.66 ppm; ESI-MS m/z : 1090.8 $[\text{M} + \text{H}]^+$; elemental analysis calcd (%) for $\text{C}_{66}\text{H}_{87}\text{N}_{15} \cdot 9\text{HCl} \cdot 2\text{H}_2\text{O}$ (1419.03 g mol^{-1}): C 55.8; H 7.3; N 11.7; found: C 56.2; H 7.6; N 11.4.

Synthesis of liposomes

Liposomes were prepared from the phospholipid 1-palmitoyl-2-oleoyl-*sn*-glycero-3-phosphocholine (POPC), 1,2-dipalmitoyl-*sn*-glycero-3-phosphoethanolamine-*N*-7-nitro-2-1,3-benzoxadiazol-4-yl (DPPE-NBD), 1,2-distearoyl-*rac*-glycerol-3-phosphoethanolamine-*N*-polyethyleneglycol-2000 (mPEG2000-DSPE) and the surfactant (Tween 80), with a molar ratio of 85/2/6/7.³⁰ The lipid mixture was dissolved in chloroform solution (5 mL) and evaporated by rotary evaporation yielding a dry lipid film and further dried under vacuum overnight.

Encapsulation of trisubstituted TPA/TPB derivatives in liposome nanoparticles. The liposome nanoparticles including the TPA/TPB derivatives were synthesised by lipid film hydration and further sonication in order to obtain unilamellar vesicles. Generally, the dry lipid film composed by POPC, mPEG2000-DSPE and DPPE-NBD was hydrated by adding an aqueous solution of TPA3P, TPA3Py, TPB3P or TPB3Py hydrochloride salts at 75 °C. Particularly, for the targeted-liposome functionalisa-

tion the aptamer AS1411 (300 μL of a 22 μM solution) was also included in the hydration step. The resulting suspension was sonicated using a probe tip sonicator and finally centrifuged (10 minutes at 3200 rpm). The non-encapsulated compound was removed from the liposome suspension by thorough dialysis in milliQ water for three days. The liposome suspension was stored at 4 °C for further studies.

Encapsulation efficiency determination. The quantification of the encapsulated TPA3P/TPA3Py/TPB3P/TPB3Py was carried out by fluorescence spectroscopy according to the TPA3P/TPA3Py/TPB3P/TPB3Py standard curves. The spectra of increasing concentrations of the ligands in MeOH:water (90:10) were recorded upon excitation at 314 nm. The emission maxima were plotted against the TPA3P/TPA3Py/TPB3P/TPB3Py concentration, obtaining a calibration curve by least-squares fitting. An aliquot of the liposome suspension under assessment was incubated 10 minutes in MeOH:water (90:10) after thorough mixing, in order to disrupt the vesicles and release the cargo. Then, the emission spectrum of the sample was registered using the same conditions used in the standard measurements. The concentration of the encapsulated TPA3P/TPA3Py/TPB3P/TPB3Py was calculated by interpolation in the calibration curve. The final obtained value and its associated error results from averaging three replicates.

Particle size characterization

DLS was used in order to estimate the particle size distribution of the liposome suspensions. The measurements were carried out in a Malvern Mastersizer 2000 equipment equilibrating the sample at 25 °C. Each experiment was performed in triplicate.

FRET melting assay

Labeled DNA was dissolved as a 20 μM stock solution in MilliQ water, then annealed as a 400 nM concentration in potassium/sodium cacodylate buffer (pH 7.3) depending on the G4 at 95 °C for 5 min, and allowed to cool slowly to room temperature overnight. The buffer used was 100 mM KCl, 10 mM LiCac. Ligands were diluted from stock solutions (see above) to final concentrations in the buffer. Each well of a 96-well plate (Applied Biosystem) was prepared with 60 μL , with a final 200 nM DNA concentration and increasing concentration of tested ligands (0–4 μM). Measurements were performed with a PCR AriaMx (Agilent Technologies) with excitation at 450–495 nm and detection at 515–545 nm. Readings were taken from 25 °C to 95 °C at an interval of 0.5 °C maintaining a constant temperature for 30 seconds before each reading. Each measurement was done in triplicate. The normalised fluorescence signal was plotted against the compound concentration and the ΔT_m values were determined.

Cell culture

MCF-7 and HeLa cells were kindly provided by the Cell Culture Section of the *Central Service for Experimental Science* (SCSIE) of the University of Valencia. LN229 cells were generously supplied by Dr Priam Villalonga (University of the Balearic Islands, Spain). Dulbecco's modified Eagle's medium (DMEM)

High Glucose, fetal bovine serum (FBS) penicillin and streptomycin were purchased from Thermo Fisher Scientific. All cell lines were grown in DMEM, which was supplemented with 10% heat-inactivated FBS (30 min, 56 °C), 100 U mL⁻¹ penicillin and 10 µg L⁻¹ streptomycin. The cultures were maintained at 37 °C in a humidified environment with 5% CO₂. The growth and proliferation of the cells were regularly checked using an optical microscope by assessment of the cell morphology, the adherent conditions and the absence of contamination.

Cell viability assays

Cell viability was determined with the 3-(4,5-dimethylthiazol-2-yl)-2,5-diphenyltetrazolium bromide (MTT) assay described previously. MTT was reduced by the mitochondrial reductase enzymes of living cells to give formazan crystals, which is directly related to the number of viable cells. Briefly, cells were seeded (4000 cells per well) in 96-well flat bottom microplates with the entire medium. After 24 hours, the medium was replaced by different ligand concentrations referring either to the free form, the encapsulated into the un-targeted liposomes or into the targeted-liposomes. Then, the cells were further exposed to 48 hours of incubation. At that point, 10 µL of a 12 mM MTT stock solution was added to each well and the plates were left to stand for 4 hours. Finally, 100 µL of DMSO were added into each well in order to dissolve the formazan crystals. The absorbance at 570 nm was measured using an ESPECTRA-MAX PLUS microplate spectrophotometer. The data analysis and the IC₅₀ calculation were performed with the Origin2017 software according to non-linear curve fitting.

Confocal laser scanning microscopy

The evaluation of the cellular uptake of liposomes was carried out using an Olympus FV1000MPE microscope. LN229 cells were plated in 65 mm plates (10 000 cells per plate) and incubated under standard conditions for 24 hours allowing the cells to adhere. Then, the medium was replaced by 2 mL of the medium containing different concentrations of both, targeted and non-targeted liposomes. In this case, liposomes do not include the ligands in order to avoid the cell death. After 1 hour of treatment, the medium was eliminated and the plates were washed with PBS, leaving finally 2 mL of PBS per well. The images were acquired by exciting at 463 nm and the emission was collected at 536 nm.

Conflicts of interest

There are no conflicts to declare.

Acknowledgements

This research was funded by the Spanish Ministry for Science and Innovation and FEDER funds from the EU (grants PID2019-110751RB-I00, PID2019-108643GA-I00, RED2018-

102331-T, MFA/2022/014 and CEX2019-000919), and the Conselleria de Innovación, Universidades, Ciencia y Sociedad Digital of the Generalitat Valenciana (CIDEGENT/2018/015 and PROMETEO Grant CIPROM/2021/030). This contribution is also based upon work from COST Action CA18202, NECTAR - Network for Equilibria and Chemical Thermodynamics Advanced Research, supported by COST (European Cooperation in Science and Technology). We especially thank Ariadna Gil Martínez for the design of the graphical abstract.

References

- (a) R. Santos, O. Ursu, A. Gaulton, A. P. Bento, R. S. Donadi, C. G. Bologa, A. Karlsson, B. Al-Lazikani, A. Hersey, T. I. Oprea and J. P. Overington, *Nat. Rev. Drug Discovery*, 2017, **16**, 19–34; (b) T. K. Kelly, D. D. De Carvalho and P. A. Jones, *Nat. Biotechnol.*, 2010, **28**, 1069–1078.
- (a) S. Neidle, *J. Med. Chem.*, 2016, **59**, 5987–6011; (b) J. Spiegel, S. Adhikari and S. Balasubramanian, *Trends Chem.*, 2020, **2**(2), 123–136; (c) J. Xu, H. Huang and X. Zhou, *JACS Au*, 2021, **1**, 2146–2216.
- (a) *Quadruplex Nucleic Acids*, ed. S. Neidle and S. Balasubramanian, RSC, Cambridge, UK, 2006; (b) *Chemistry and Biology of Non-Canonical Nucleic Acids*, ed. N. Sugimoto, Wiley-VCH, 2021.
- (a) V. S. Chambers, G. Marsico, J. M. Boutell, M. D. Antonio, G. P. Smith and S. Balasubramanian, *Nat. Biotechnol.*, 2015, **33**, 877–881; (b) R. Hänsel-Hertsch, D. Beraldi, S. V. Lensing, G. Marsico, K. Zyner, A. Parry, M. D. Antonio, J. Pike, H. Kimura, M. Narita, D. Tannahill and S. Balasubramanian, *Nat. Genet.*, 2016, **48**, 1267–1272; (c) A. Bedrat, L. Lacroix and J. L. Mergny, *Nucleic Acids Res.*, 2016, **44**, 1746–1759.
- (a) D. Rhodes and H. J. Lipps, *Nucleic Acids Res.*, 2015, **43**, 8627–8637; (b) D. Varshney, J. Spiegel, K. Zyner, D. Tannahill and S. Balasubramanian, *Nat. Rev. Mol. Cell Biol.*, 2020, **21**, 459–474.
- (a) S. Neidle, *J. Med. Chem.*, 2016, **59**, 5987–6011; (b) E. Palma, J. Carvalho, C. Cruz and A. Paulo, *Pharmaceuticals*, 2021, **14**, 605; (c) N. Kosiol, S. Juranek, P. Brossart, A. Heine and K. Paeschke, *Mol. Cancer*, 2021, **20**, 40; I. Alessandrini, M. Recagni, N. Zaffaroni and M. Folini, *Int. J. Mol. Sci.*, 2021, **22**, 5947.
- (a) Y. Yan, J. Tan, T. Ou, Z. Huang and L. Gu, *Expert Opin. Ther. Pat.*, 23(11), 1495–1509; (b) <https://clinicaltrials.gov/ct2/show/NCT02267863>; (c) <https://clinicaltrials.gov/ct2/show/NCT00780663>; (d) <https://clinicaltrials.gov/ct2/show/NCT02719977>.
- (a) E. Mendes, I. M. Aljnadi, B. Bahls, B. L. Victor and A. Paulo, *Pharmaceuticals*, 2022, **15**(3), 300; (b) D. Monchaud and M. P. Teulade-Fichou, *Org. Biomol. Chem.*, 2008, **6**, 627–636.
- (a) S. Neidle, *Pharmaceuticals*, 2022, **15**, 7; (b) T. M. Ou, Y. J. Lu, J. H. Tan, Z. S. Huang, K. Y. Wong and L. Q. Gu,

- 1 *ChemMedChem*, 2008, **3**, 690–713; G. W. Collie and
2 **Q16** G. N. Parkinson, *Chem. Soc. Rev.*, 2011, **40**, 5867.
- 10 (a) J. Carvalho, J. L. Mergny, G. F. Salgado, J. A. Queiroz
and C. Cruz, *Trends Mol. Med.*, 2020, **26**(9), 848–861;
5 (b) Q. Cao, Y. Li, E. Freisinger, P. Z. Qin, R. K. O. Sigel and
Z. W. Mao, *Inorg. Chem. Front.*, 2017, **4**(1), 10–32;
(c) S. N. Georgiades, N. H. Karim, K. Suntharalingam and
R. Vilar, *Angew. Chem., Int. Ed.*, 2010, **49**(24), 4020–4034.
- 11 (a) Z. A. E. Waller, P. S. Shirude, R. Rodriguez and
S. Balasubramanian, *Chem. Commun.*, 2008, **44**, 1467–1469;
10 (b) Z. A. E. Waller, S. A. Sewitz, S. T. D. Hsu and
S. Balasubramanian, *J. Am. Chem. Soc.*, 2009, **131**(35),
12628–12633; (c) N. M. Smith, G. Labrunie, B. Corry,
15 P. L. T. Tran, M. Norret, M. Djavaheri-Mergny, C. L. Raston
and J. L. Mergny, *Org. Biomol. Chem.*, 2011, **9**(17), 6154–
6162.
- 12 L. Y. Liu, W. Liu, K. N. Wang, B. C. Zhu, X. Y. Xia, L. N. Ji
and Z.-W. Mao, *Angew. Chem., Int. Ed.*, 2020, **59**, 9719–9726.
- 20 13 Z. Tan, Y. Hao and K. Zheng, *Biochem. Biophys. Res.
Commun.*, 2020, **531**, 84–87.
- 14 J. Lopes-Nunes, P. A. Oliveira and C. Cruz, *Pharmaceuticals*,
2021, **14**(7), 671.
- 15 (a) M. J. Webber and R. Langer, *Chem. Soc. Rev.*, 2017, **46**,
6600–6620; (b) D. Peer, J. M. Karp, S. Hong,
25 O. C. Farokhzad, R. Margalit and R. Langer, *Nat.
Nanotechnol.*, 2007, **2**, 751–760; (c) J. K. Patra, G. Das,
L. F. Fraceto, E. V. R. Campos, M. P. Rodriguez-Torres,
L. S. Acosta-Torres, L. A. Diaz-Torres, R. Grillo,
30 M. K. Swamy, S. Sharma, S. Habtemariam and H. S. Shin,
J. Nanobiotechnol., 2018, **16**, 71; (d) J. I. Hare, T. Lammers,
M. B. Ashford, S. Puri, G. Storm and S. T. Barry, *Adv. Drug
Delivery Rev.*, 2017, **108**, 25–38.
- 35 (a) T. M. Allen and P. R. Cullis, *Adv. Drug Delivery Rev.*,
2013, **65**, 36–48; (b) L. Sercombe, T. Veerati, F. Moheimani,
S. Y. Wu, A. K. Sood and S. Hua, *Front. Pharmacol.*, 2015, **6**,
286; (c) D. Guimaraes, A. Cavaco-Paulo and E. Nogueira,
Int. J. Pharm., 2021, **601**, 120571.
- 40 17 (a) Y. Barenholz, *J. Controlled Release*, 2012, **160**, 117–134;
(b) V. Makwana, J. Karanjia, T. Haselhorst, S. Anoopkumar-
Dukie and S. Rudrawar, *Int. J. Pharm.*, 2021, **593**, 120117.
- 18 (a) U. Bulbake, S. Doppalapudi, N. Kommineni and
W. Khan, *Pharmaceutics*, 2017, **9**, 12; (b) B. S. Pattni,
45 V. V. Chupin and V. P. Torchilin, *Chem. Rev.*, 2015, **115**,
10938–10966.
- 19 E. Blanco, H. Shen and M. Ferrari, *Nat. Biotechnol.*, 2015,
33, 941–951.
- 20 I. Pont, A. Calatayud-Pascual, A. López-Castellano,
1 E. P. Albelda, E. García-España, L. Martí-Bonmatí,
J. C. Frias and M. T. Albelda, *PLoS One*, 2018, **13**, e0190540.
- 21 (a) F. Hammerer, F. Poyer, L. Fourmois, S. Chen, G. Garcia,
5 M. P. Teulade-Fichou, P. Maillard and F. Mahuteau-Betzer,
Bioorg. Med. Chem., 2018, **26**, 107–118; (b) G. Bordeau,
R. Lartia, G. Metge, C. Fiorini-Debuisschert, F. Charra and
M. P. Teulade-Fichou, *J. Am. Chem. Soc.*, 2008, **130**, 16836–
16837; (c) M. Q. Wang, Z.-Y. Wang, Y. F. Yang, G. Y. Ren,
10 X. N. Liu, S. Li, J. W. Wei and L. Zhang, *Tetrahedron Lett.*,
2017, **58**, 3296–3300; (d) M. Q. Wang, L. X. Gao, Y. F. Yang,
X. N. Xiong, Z. Y. Zheng, S. Li, Y. Wu and L. L. Ma,
Tetrahedron Lett., 2016, **57**, 5042–5046.
- 22 I. Pont, A. Martínez-Camarena, C. Galiana-Roselló,
15 R. Tejero, M. T. Albelda, J. González-García, R. Vilar and
E. García-España, *ChemBioChem*, 2020, **21**, 1167–1177.
- 23 I. Pont, J. González-García, M. Inclán, M. Reynolds,
E. Delgado-Pinar, M. T. Albelda, R. Vilar and E. García-
España, *Chem. – Eur. J.*, 2018, **24**, 10850–10858.
- 20 24 (a) P. J. Bates, D. A. Laber, D. M. Miller, S. D. Thomas and
J. O. Trent, *Exp. Mol. Pathol.*, 2009, **86**, 151–164; (b) Z. Cao,
R. Tong, A. Mishra, W. Xu, G. C. L. Wong, J. Cheng and
Y. Lu, *Angew. Chem., Int. Ed.*, 2009, **48**, 6494–6498.
- 25 (a) P. J. Bates, E. M. Reyes-Reyes, M. T. Malik,
E. M. Murphy, M. G. O’Toole and J. O. Trent, *Biochim.
Biophys. Acta*, 2017, **1861**, 1414–1428; (b) E. M. Reyes-Reyes,
Y. Teng and P. J. Bates, *Cancer Res.*, 2010, **70**, 8617–8629.
- 30 26 (a) B. Meckes, R. J. Banga, S. T. Nguyen and C. A. Mirkin,
Small, 2018, **14**, 1702909; (b) J. R. Ferrer, A. J. Sinagra,
D. Ivancic, X. Y. Yeap, L. Qiu, J. J. Wang, Z. J. Zhang,
J. A. Wertheim and C. A. Mirkin, *ACS Nano*, 2020, **14**, 1682–
1693.
- 35 27 (a) J. Carvalho, A. Paiva, M. P. C. Campello, A. Paulo,
J.-L. Mergny, G. F. Salgado, J. A. Queiroz and C. Cruz, *Sci.
Rep.*, 2019, **9**, 7945; (b) J. Figueiredo, J. Lopes-Nunes,
J. Carvalho, F. Antunes, M. Ribeiro, M. P. C. Campello,
A. Paulo, A. Paiva, G. F. Salgado, J. A. Queiroz, J.-L. Mergny
and C. Cruz, *Int. J. Pharm.*, 2019, **568**, 118511.
- 40 28 J. S. Suk, Q. Xu, N. Kim, J. Hanes and L. M. Ensign, *Adv.
Drug Delivery Rev.*, 2016, **99**, 28–51.
- 29 Z. Gong, B. Yang, H. Lin, Y. Tang, Z. Tang, J. Zhang,
H. Zhang, Y. Li, Y. Xie, Q. Li and L. Chi, *ACS Nano*, 2016,
45 **10**(4), 4228–4235.
- 30 K. Kimpe, T. N. Parac-Vogt, S. Laurent, C. Piérart, L. V. Elst,
R. N. Muller and K. Binnemans, *Eur. J. Inorg. Chem.*, 2003,
3021–3027.